Korean J. Chem. Eng., 32(12), 2492-2500 (2015)
DOI: 10.1007/s11814-015-0105-z

pISSN: 0256-1115
eISSN: 1975-7220

Surface modification of poly(vinylidene fluoride) membrane with hydrophilic and anti-fouling performance via a two-step polymerization

Gui-E Chen*, Li Sun*, Zhen-Liang Xu,†, Hu Yang**, Hui-Hong Huang*, and Yan-Jun Liu***

*School of Chemical and Environmental Engineering, Shanghai Institute of Technology,
100 Haiquan Road, Shanghai 201418, China
**State Key Laboratory of Chemical Engineering, Membrane Science and Engineering R&D Lab.,
Chemical Engineering Research Center, East China University of Science and Technology,
130 Meilong Road, Shanghai 200237, China
(*Received 3 January 2015 • accepted 16 May 2015*)

Abstract−The surface modification of poly (vinylidene fluoride) (PVDF) membrane was performed via a two-step polymerization reactions. Poly (acrylic acid) (PAAc) was first grafted onto the membrane surface for the preparation of PVDF-g-PAAc membrane, and then poly (ethylene glycol) 200 (PEG 200) was immobilized on the membrane surface by the esterification reaction for the fabrication of PVDF-g-PEGA membrane. Attenuated total reflectance (ATR) FTIR, X-ray photoelectron spectroscopy (XPS), scanning electron microscope (SEM), and protein adsorption, water flux, water content and dynamic contact angle were conducted to characterize the structures and performance of the resultant PVDF membranes. The experimental results showed that the adsorption of bovine serum albumin (BSA) on the PVDF-g-PEGA membrane decreased about 80% when the grafting ratio reached to 15 wt%, compared with the pristine PVDF membrane. Moreover, the water contact angle of the membrane dropped to 60.5°, while the membrane pore sizes remained little changed.

Keywords: Poly(Vinylidene Fluoride), Surface Modification, Hydrophilic, Anti-fouling, Polymerization

INTRODUCTION

Poly (vinylidene fluoride) (PVDF), a semicrystalline polymer, has gained increasing attention owing to its outstanding thermal and chemical resistance, good conductivity and mechanical strength in the membrane industry [1,2]. In addition to the applications in microfiltration (MF), ultrafiltration (UF) and nanofiltration (NF), PVDF membrane is also used in membrane distillation, gas separation, pervaporation, and recovery of biofuels, separator for lithium ion battery, ion exchange process and others [3-6]. However, due to its inherent hydrophobicity and low surface energy, PVDF membranes are easily fouled in aqueous solutions like biomedical filtration and protein separation processes, which could reduce the membrane efficiency, shorten the membrane lifespan and increase the operation cost [7,8]. It is well known that a hydrophilic surface can effectively resist the membrane fouling. Therefore, considerable efforts have been devoted to obtain the hydrophilic PVDF membranes by surface modification or blending [9-11].

Blending modification is an extensively applied approach to endow hydrophilicity and anti-fouling properties on the PVDF membranes by adding hydrophilic or amphiphilic polymers during the membrane fabrication [12-16]. Hashim et al. [14] prepared hydrophilic PVDF membranes from amphiphilic copolymer poly(ethylene glycol) methyl ether methacrylate (PEGMA) (PVDF-g-PEGMA). These obtained membranes showed a significant improvement of hydrophilicity and fouling resistance. The surface modification mainly includes coating and grafting. Boributh et al. [17] studied the modification of PVDF membrane with chitosan solution. It was found that the chitosan deposited on the membrane can effectively reduce the protein fouling and increase the hydrophilicity. Li et al. [18] prepared PVDF membrane using physisorbed free radical grafting technique. These membranes exhibited high hydrophilic and low-protein fouling performance after grafting zwitterionic monomer sulfobetaine methacrylate (SBMA). Among these modification methods, surface grafting has attracted much interest due to its obvious modification effect. To incorporate the desired properties onto the membrane, the PVDF membrane surfaces have to be pretreated to provide active sites or groups prior to graft polymerization. Activation techniques like plasma treatment [19], ozonization [20], and UV irradiation [21] are all expensive and require specific equipment. Therefore, a simple and facile activation method for the modification of PVDF membrane is of urgent requirement.

According to Brewis et al. [22] and Ross et al. [23], the conjugated double bond and polyenes structure generated on the membrane surface by exposure to the alkaline solution can be attacked with specific reactants to introduce proper functional groups. Therefore, the PVDF membrane was pretreated with alkaline before grafting polymerization in this study. This simple and effective initiation process can provide enough active sites for the following reactions. Meanwhile, the membranes could retain the excellent bulk properties of a hydrophobic material. As a strong hydrophilic substance, acrylic acid (AAc) has gained extensive attention in the hydrophilic

†To whom correspondence should be addressed.
E-mail: chemxuzl@ecust.edu.cn

modification of PVDF membrane, and several research groups have evaluated the anti-fouling performance and hydrophilicity of AAc on the membrane [24-26]. In general, the formation of PAAc chains on the membrane surface could lead to the sharp decline of the water flux due to the blocking of the membrane pores. To suppress the extent of the decreased water flux, PVDF membranes will be further modified by introducing lager hydrophilic groups or polymers, like polyethylene glycol (PEG). PEG is an ideal antifouling material used in membrane modification due to its hydrophilicity, large excluded volume of the hydrated PEG chains [27-29]. Wang et al. [27] immobilized PEG chains onto the surfaces of PVDF microporous membranes. It was found that the protein adsorption on the PEG-g-PVDF membrane was decreased with the grafting of PEG.

In this work, a facile and simple two-step grafting polymerization reaction is carried out for the surface modification of PVDF membrane. First, PAAc chains are grafted onto the PVDF membrane with surface-initiated grafting polymerization after alkaline pretreatment. Then PEG is grafted onto the PVDF-g-PAAc membrane through the esterification reaction of the carboxyl group in PAAc with the hydroxyl group in PEG. Expertly, our modified PVDF membranes exhibit a significant improvement of hydrophilicity and anti-fouling performance. The filtration performance, anti-fouling properties and dynamic contact angles of the modified membranes are characterized.

EXPERIMENTAL

1. Materials

Poly (vinylidene fluoride) (PVDF) membrane, with an average pore diameter of 0.45 μm was provided by Merck Millipore Company. Acrylic acid (AAc), poly (ethylene glycol) (PEG 200, Mn= 200), ethanol, 1-propyl alcohol, benzoyl peroxide (BPO), potassium hydroxide (KOH) and hydrochloric acid (HCl, 37 wt%) were purchased from Shanghai Sinopharm Chemical Reagent Co. LTD (China). Bovine serum albumin (BSA) (MW=67 K) was obtained from Lianguan Biochemical Reagent Company of Shanghai. Deionized water was supplied by our own lab. BPO was recrystallized from pure trichloromethane and methanol before use. HCl aqueous solution was diluted to 10 wt%. All other chemicals used for experiments were analytical grade and were used directly.

2. Alkaline Pretreatment

PVDF membranes were immersed in different concentrations of KOH aqueous solution, ethanol solution and ethanol/water (W/W, 1/1 and 95/5) solutions at 50-80 °C; after a certain treatment time, the membranes were taken out and washed to neutral (pH=7) with the plenty of deionized water. The purpose of the alkaline treatment is to produce the activated carbon conjugated double bonds on the membranes [30,31].

3. Preparation of PVDF-g-PAAc Membrane

The effect of three kinds of alkaline treatment system on the grafting ratio of PVDF membrane was evaluated. According to experimentation and data comparison, the optimum condition of alkaline pretreatment was ethanol/water (1 : 1, mass ratio) solution consisting of 10 wt% KOH at 60 °C. The PVDF-g-PAAc membrane was prepared first by immersing unmodified PVDF membrane into an ethanol/water (1 : 1, mass ratio) solution consisting of 10 wt% KOH at 60 °C; after a certain treatment time, ranging from 0.5 to 3 h, the membrane was taken out and washed to neutral. Subsequently, the PVDF membrane suffering from alkaline treatment was put into a 1-propyl alcohol solution containing 8 wt% AAc and 1 wt% BPO in a sealed conical flask; the reaction was carried out at 70 °C for four hours. The grafted PVDF membrane was then exhaustively washed in an ultrasonic cleaner to clear away the physically-adsorbed polymers. The grafting ratio of PAAc was calculated gravimetrically as follows:

$$G_R = \frac{W_1 - W_0}{W_0} \times 100 \text{ wt\%} \quad (1)$$

where W_1 indicates the weight of PVDF-g-PAAc membrane, and W_0 indicates the weight of membrane after the alkaline treatment.

4. Preparation of PVDF-g-PEGA Membrane

The PVDF-g-PAAc membranes with various grafting ratios (G_R) were immersed into the esterification solutions of PEG 200, containing 1 wt% HCl as the catalyst. The reactions were at 105 °C for different periods, including 1, 2, 3, 4 h, respectively. The resultant PVDF membranes were then rinsed with deionized water thoroughly to remove the unreacted residual PEG.

All the above solutions containing membranes were degassed through ultrasonic.

5. Characterization of Structures and Morphologies

The surface chemical structures of the original and modified membranes were investigated by ATR-FTIR and XPS. ATR-FTIR was conducted on a Thermo Nicolet 360 (American) instrument and each spectrum was captured via 32 scans at a resolution of 4 cm^{-1}; the range of the spectra was from 500 to 4,000 cm^{-1}. XPS analysis was performed on a Kratos AXIS Ultra HAS spectrometer with a monochromatized Al K radiation (1,486.6 eV). The surface and the cross-sectional morphologies of the modified and initial membranes were observed by scanning electronic microscopy (SEM, S-3400N, Hitachi). The membranes were frozen in liquid nitrogen, fractured into small samples to obtain the cross-sections. Samples for SEM analysis were sputtered with gold-palladium alloy prior to microscopic analysis.

6. Characterization of Pore Size, Rejection and Water Content

The maximum pore size of the membrane was determined by the bubble point using a DJ-5 membrane and filter integrity test instrument, manufactured by Shanghai Jingyuan Filter Equipment Co., Ltd. (China). The membrane sample was thoroughly wetted with ethanol before measurement. Then the membrane sample was transferred into a test instrument which connected a gas source; when the gas passed through the wetted membrane, the gas pressure would equal to the interfacial tension of the liquid within the membrane pores at a moment, and the gas pressure at this point, namely bubble point, corresponding to the maximum pore size of the membrane. The result was obtained as follows:

$$D = \frac{4 \times \gamma \times B \times \cos\theta}{P} = \frac{C \times \gamma}{P} \quad (2)$$

where D is the diameter of the membrane pores; γ is the interfacial tension of the liquid; P is the gas pressure; θ is the contact angle between the liquid and the wall of pores; B is capillary constant; C

is constant. In this study, the used liquid is ethanol. $\gamma_{ethanol}$ is 22.3 mN/m; θ is 0; B is 1; the unit of P is Pa; Therefore, Eq. (2) is derived as follows:

$$D(\mu m)=\frac{8.92\times10^{4}}{P} \quad (3)$$

The rejection of the membrane was characterized using polystyrene microspheres (3×10^{-5} g/ml, 713.3 nm, Lot No.: PS-M-11003), provided by Wuhan Branch Micro-Technology Co., Ltd. (China). The measuring method was the same as the following water flux, and the concentrations of the feed and permeates were determined via a UV spectrophotometer at 338 nm. The rejection (R) was calculated by the following equation [32]:

$$R=\left(1-\frac{c_p}{c_f}\right)\times100\ wt\% \quad (4)$$

where c_p and c_f are solute concentrations of permeate and feed solutions, respectively.

The membrane hydrophilicity can be evaluated by the water content of the membrane. The PVDF membrane was first dried at 80 °C for 4 h to a constant weight; the weight was marked as W_F. Then the membrane was immersed in deionized water for 24 h at room temperature. The membrane was then removed and the surface water was wiped dry with filter paper; the membrane weight was then recorded as W_G. The water content of the membrane was calculated by[33]:

$$\text{Water content}=\frac{w_G-w_F}{w_F}\times100\ wt\% \quad (5)$$

7. Characterization of Protein Adsorption

A BSA solution with a concentration of 2 mg/ml was used to study the adsorption of the BSA of the nascent and modified membrane. The membrane sample with efficient surface area of 12.56 cm^2 was first washed with ethanol, followed by washing with water. After that, the sample was transferred into a tube filled with 10 ml BSA solution for 24 h at 30 °C. Then, the sample was taken out. The BSA concentration of the solution was determined by a total organic carbon analyzer (TOC, Model TOC_{VPN}, Shimadzu, Japan). The amount of protein adsorption (C_{ad}) of the membrane could be calculated as follows:

$$C_{ad}=\frac{(C_i-C_a)\times V}{A} \quad (6)$$

where the parameters C_i and C_a denote the BSA concentration before and after membrane adsorption, V is the volume of the soaking solution and A is the efficient surface area of the PVDF membrane.

8. Filtration Performance

The filtration performance of the pristine and modified PVDF membrane was measured by a self-made MF experimental equipment. A circular cut membrane with constant membrane area (A= 2.826×10^{-3} m^2) was placed into a cell, and the pressure in the cell was kept at 1 bar. Afterwards, pure water and BSA solution (2 mg/ml) were forced to permeate through the membrane for a due course of time alternately, and the flux was marked as $J_{w(R)}$. Protein fouling experiments were conducted by immersing the membranes in 10 mg/ml BSA solutions for 24 h at 25 °C. Then the membranes were taken out from the solutions and rinsed with the deionized water several times. The water flow rates (J_R) of the membrane after protein fouling were measured with the method mentioned above. Each membrane sample was pressurized with distilled water for half an hour before the filtration experiment. The fluxes were calculated by [34]:

$$J_{W(R)}=\frac{V_{W(R)}}{A\times\Delta t} \quad (7)$$

where $V_{W(R)}$ is the permeate volume, A=2.826×10^{-3} m^2, is the membrane area, and Δt is the permeation time.

9. Characterization of Dynamic Contact Angle

The dynamic contact angle (θ) of the PVDF membrane was measured by JC20 00D1 (produced by Shanghai Zhongcheng Digital Technology Apparatus Co. Ltd., China) at ambient temperature. A droplet of 0.2 μL water was dropped from a needle tip onto the membrane surface. The machine was equipped with a camera enabling image capture at 10 frames/s. Contact angles were calculated from these images using the specific calculation software. To ensure that the results were fully authentic, the experimental errors in measuring the θ values were evaluated to be less than ± 0.5°. Each set of sample was measured in triplicate, and the average data of the contact angle was used.

RESULTS AND DISCUSSION

1. Surface Modification and Characterization of PVDF Membrane

The PVDF-g-PEGA membrane was prepared via a two-step grafting polymerization, which is illustrated in Fig. 1. In the first step, PAAc chains were grafted onto the PVDF membrane with the sur-

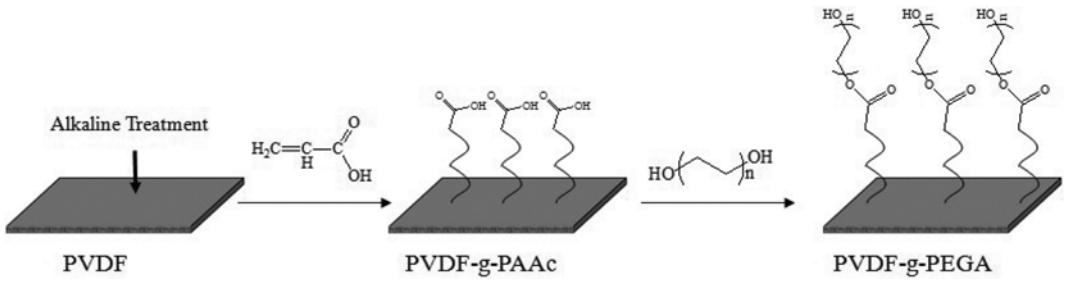

Fig. 1. Schematic illustration for the modification process of PVDF membrane.

face-initiated grafting polymerization after alkaline pretreatment. Then, PEG 200 was introduced onto the PVDF-g-PAAc membrane through the esterification reaction between the -COOH groups of the PAAc and the -OH groups of the PEG 200. The results are summarized in Table 2. The presence of PAAc chains and the subsequent esterification groups on the PVDF membrane are confirmed by ATR-FTIR spectra. The spectra of the original PVDF membrane, the PVDF-g-PAAc membrane (GA, Table 2) and the PVDF-g-PEGA membrane (G4, Table 2) are shown in Fig. 2. After the grafting of PAAc, the presence of PAAc chains could be confirmed from the absorption peak appearing at 1,720 cm^{-1}, which is associated with the -COOH stretching. For the membrane of PVDF-g-PEGA, the obvious absorption band at 1,731 cm^{-1}, correlated with O-C=O stretching, is observed clearly. Meanwhile, the characteristic peak appearing at 1,110 cm^{-1} is attributed to the stretching of C-O-C in PEG. Therefore, the spectra of the surface modified PVDF membranes preliminarily indicate that the PEGA chains are successfully grafted on the surface of the PVDF membrane.

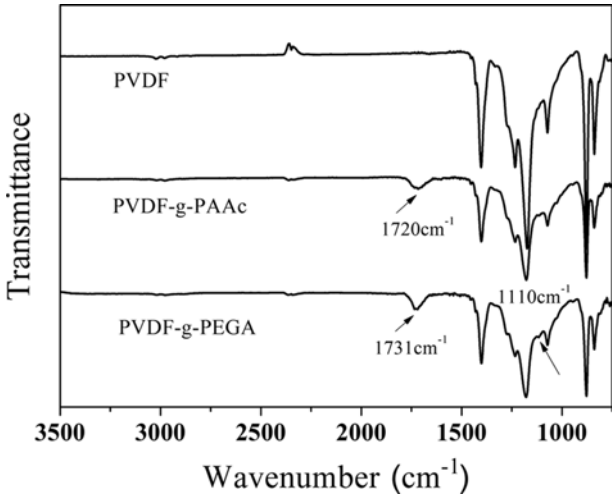

Fig. 2. ATR-FTIR spectra of the pristine and surface modified PVDF membrane.

To further demonstrate the presence of the graft copolymers onto the PVDF membrane, X-ray photoelectron spectroscopy (XPS) analysis was used to investigate the chemical components of the pristine and modified membranes. The wide-scan and C1s characteristic peaks of the membranes in XPS spectra are given in Fig. 3. The background was subtracted from the XPS spectra by using a Shirley-type background subtraction. Only C1s and F1s characteristic peaks exist in the pristine PVDF membrane (Fig. 3(a)). For the PVDF-g-PAAc and PVDF-g-PEGA membrane, the emergence of O1s characteristic peaks and the increase of the C/F ratio in the wide-scan spectra demonstrate that PAAc and PEGA chains are chemically grafted onto the PVDF membrane. The surface elemen-

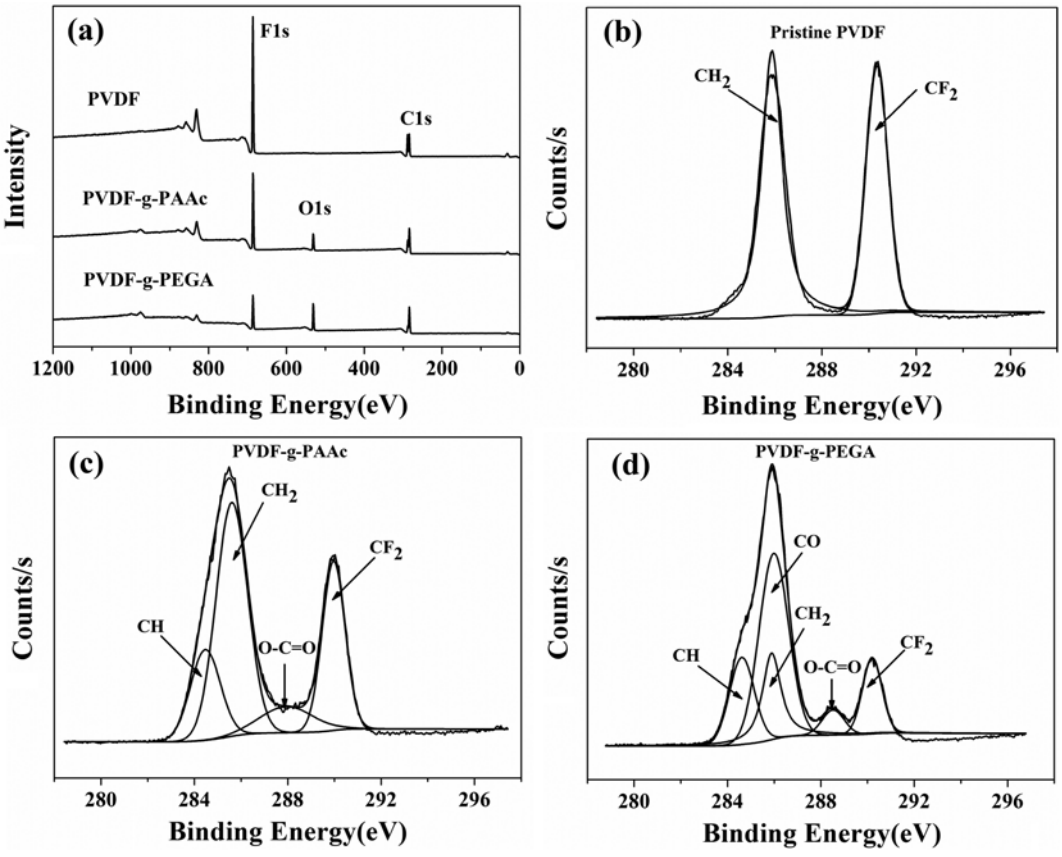

Fig. 3. XPS wide-scan spectra (a) and C1s core-level spectra of (b) pristine PVDF membrane; (c) PVDF-g-PAAc membrane (G_R=15 wt%); (d) PVDF-g-PEGA membrane (G4, Table 2).

Table 1. Elemental compositions of pristine and modified PVDF membrane

Membrane sample	Atom percent (%)		
	C1s	O1s	F1s
PVDF	49.43	0	50.57
PVDF-g-PAAc	54.69	10.54	34.77
PVDF-g-PEGA	58.77	15.71	25.52

tal compositions of the PVDF membranes are summarized in Table 1. An obviously increase of the oxygen element can be seen in the surface modified PVDF membrane. The low ratio of C/F in the pristine PVDF membrane could be ascribed to the restricted sampling location in XPS measurement. Moreover, the chemical structures of the membranes are further analyzed by C1s core-level spectra. The pristine PVDF membrane shows two peaks (Fig. 3(b)), with the binding energy at 285.8 eV for -CH_2 and 290.5 eV for -CF_2, respectively, which are in perfect accordance with the data reported by Hsu et al. [35]. Compared with those of pristine PVDF membrane, the PVDF-g-PAAc membrane (Fig. 3(c)) exhibits characteristic peaks at 284.6 eV for -CH species and 288.5 eV for O-C=O species, which confirms the presence of PAAc chains. Fig. 3(d) shows the C1s core-level spectrum of the PVDF-g-PEGA membrane. Unlike the result of the PVDF-g-PAAc membrane, the intensive absorption peaks at 286.2 eV for -CO species of PEG chains could observed clearly, and the presence of the PEG chains could also be confirmed by the reduction of the intensity for -CF_2 species. Therefore, the results of ATR-FTIR and XPS indicate the successful preparation of PVDF-g-PEGA membranes.

The surface morphologies of the original and surface modified PVDF membranes are obtained at the magnification of ×3000 and ×5000 in Fig. 4. The original PVDF membrane shows a homogeneous porous structure. After the grafting of PAAc and PEG, the membrane pore size is reduced and the porous structure becomes heterogeneous. It indicates that the formation of PAAc and PEGA could roughen the layer of the membrane. The cross-sectional morphologies of the original and surface modified PVDF membranes are shown in Fig. 5. Compared with the uniform porous structure of the pristine PVDF membrane, the PVDF-g-PAAc and PVDF-g-PEGA membranes exhibit thickened porous structure due to the coverage of PAAc and PEGA chains. The cross-sectional micrographs of surface modified membranes indicate that the grafted chains have incorporated not only onto the membrane surface, but also into the pores of the membrane surface.

2. Characterization of Pore Size, Rejection and Water Content of the Membrane

As shown in Table 2, the maximum pore size, corresponding to the bubble point, exhibits a substantial decrease for the PVDF-g-PAAc membrane, which is caused by the fact that the graft layer of PAAc covered the membrane pores. In contrast, the maximum pore size of the PVDF-g-PEGA membrane exhibits an increased tendency. Possible explanation is that the degree of the membrane pore clogging was reduced after introducing the PEG 200 onto the membrane surface with the esterification reaction. Overall, the maximum pore size (0.440-0.528 μm) of the PVDF membranes remains little changed. The rejection of the modified PVDF membrane is also similar to that of original one, which indicates that the surface modification of PVDF membrane shows little effect on the membrane pore structure.

The water content of the membrane is also one of the important parameters of the hydrophilicity of the membrane. The PVDF-g-PAAc membrane exhibits high water content due to the large amount of hydrophilic carboxyl groups. Meanwhile, the water content of the membranes increases with the increase of the grafting ratio, indicating that the hydrophilicity of the surface modified PVDF membranes has been greatly improved. The water content of the membranes with various esterification reaction times in Table 3 shows little change. This is because the PAAc modified PVDF membrane exhibits excellent hydrophilicity, and the effect of the introduction of the hydroxyl groups on the hydrophilicity appears negligible.

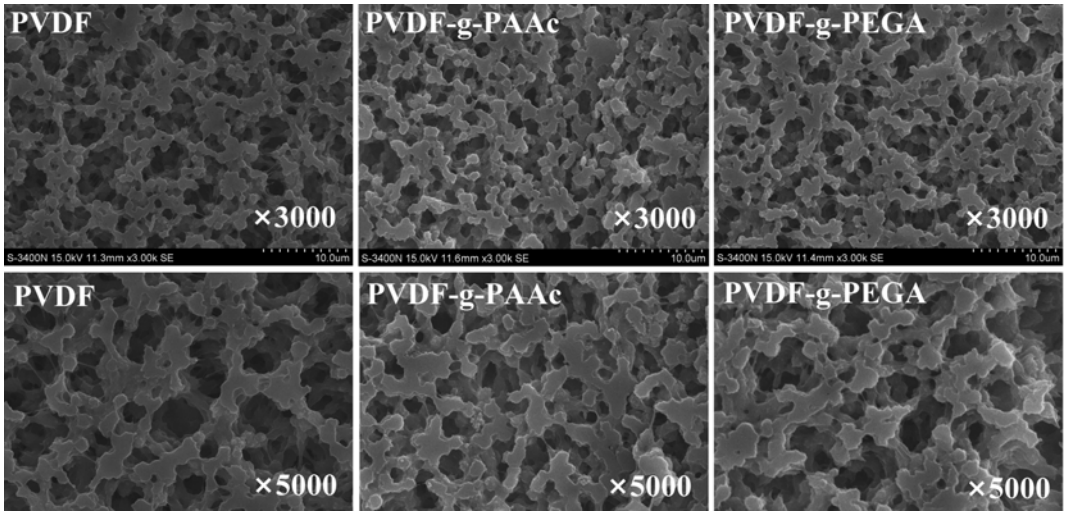

Fig. 4. Surface morphologies of the original PVDF membrane, the PVDF-g-PAAc membrane (G_R=15 wt%) and the PVDF-g-PEGA membrane (G4, Table 2).

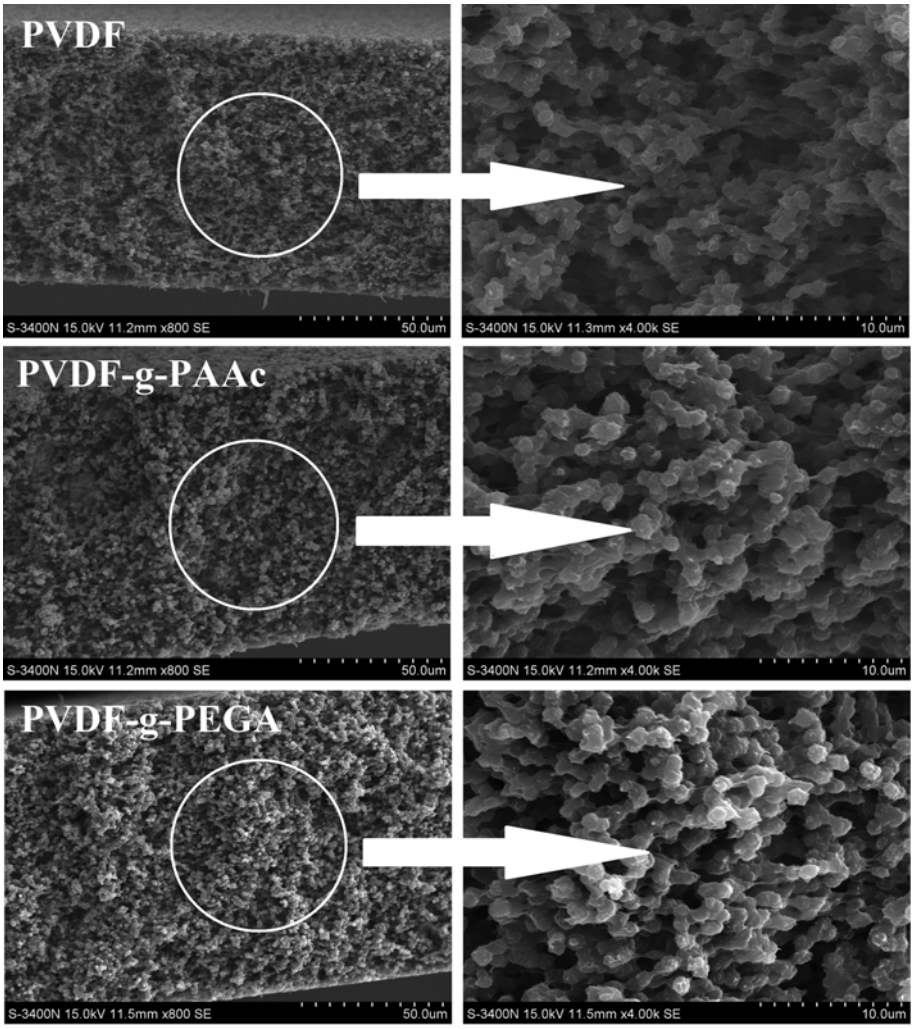

Fig. 5. Cross-sectional morphologies of the original PVDF membrane, the PVDF-g-PAAc membrane (G_R=15 wt%) and the PVDF-g-PEGA membrane (G4, Table 2).

Table 2. Performance of the pristine and modified PVDF membranes

Membrane number	Sample	Alkaline treatment time/(h)	Graft ratio/ (%)	Bubble point/ (MPa)	Maximum pore size, D/mm	Water content (%)	Rejection/ (R, %)	Water flux/ ($L/m^2/h$)
G0	PVDF	0	0	0.169±0.027	0.528±0.084	0	92.0±1.8	1260±13.8
GA	PVDF-g-PAAc	2.0	15	0.208±0.041	0.429±0.085	98.0±2.0	95.8±1.2	1060±12.1
G1	PVDF-g-PEGA	0.5	4.0	0.191±0.031	0.467±0.077	76.8±2.5	93.5±0.5	1200±12.8
G2	PVDF-g-PEGA	1.0	7.0	0.193±0.034	0.463±0.082	80.6±1.5	94.6±1.0	1180±11.2
G3	PVDF-g-PEGA	1.5	9.8	0.196±0.045	0.455±0.087	85.0±2.7	95.2±1.5	1170±11.5
G4	PVDF-g-PEGA	2.0	15	0.203±0.039	0.440±0.082	89.3±5.2	95.5±1.5	1160±12.7
G5	PVDF-g-PEGA	3.0	16.9	0.194±0.035	0.460±0.083	92.6±3.9	94.0±2.2	1170±13.5

Table 3. Performance of PVDF-g-PEGA membranes

Membrane number	Sample	Alkaline treatment time/(h)	Graft ratio/ (%)	Esterification reaction time/(h)	Bubble point/ (MPa)	Maximum pore size, D/mm	Water content/(%)	Rejection/ (R, %)
R1	PVDF-g-PEGA	2.0	15	1.0	0.194±0.035	0.460±0.083	89.0±5.0	94.0±1.0
R2	PVDF-g-PEGA	2.0	15	2.0	0.192±0.033	0.465±0.080	88.5±4.9	93.8±1.2
R3	PVDF-g-PEGA	2.0	15	3.0	0.189±0.030	0.472±0.075	89.0±5.0	93.5±1.6
R4(G4)	PVDF-g-PEGA	2.0	15	4.0	0.203±0.039	0.440±0.082	89.3±5.2	95.5±1.5

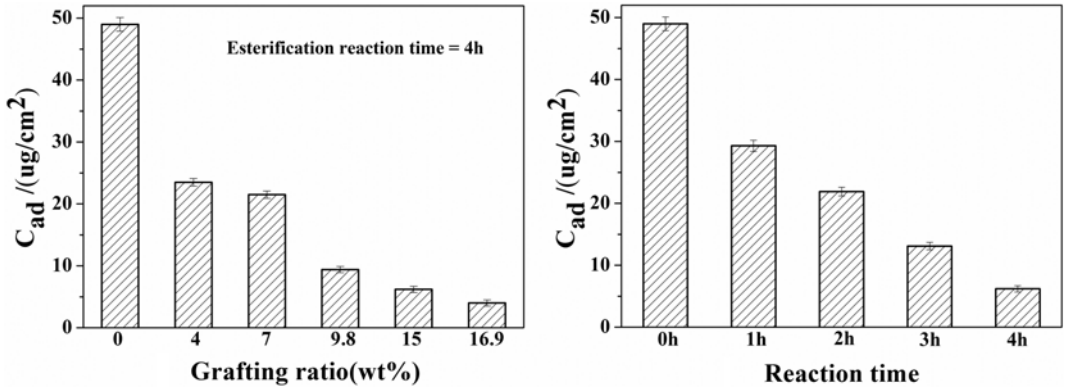

Fig. 6. Protein adsorption of pristine and surface modified membranes with various grafting ratio and esterification reaction time.

3. Filtration Performance of the Surface Modified Membranes

The anti-fouling performance of the surface modified PVDF membranes is evaluated by protein adsorption and filtration performance after protein fouling. Fig. 6 shows the effect of various grafting ratio (esterification reaction time=4 h) and esterification reaction time (G_R=15 wt%) on the membrane protein adsorption. It is found that the amount of protein adsorption on the membrane is decreased with the increase of the grafting ratio and esterification reaction time. The amount of BSA adhered to the pristine PVDF membrane is 49 μg/cm^2, while it is only about 10 μg/cm^2 for the surface modified membrane. The PVDF-g-PEGA membrane with the grafting ratio of 16.9 wt% shows the best anti-fouling property (4 μg/cm^2). Possible interpretation for the resistance of protein adsorption on the modified membrane is that the grafted PEGA chains on the membrane formed a hydration layer on the hydrophilic surface. With the amount of the grafted PEGA chains increasing, the strengthened hydration interaction can effectively prevent protein adherence.

The water flux data in Fig. 7 shows the anti-fouling performance of the pristine PVDF membrane and the PVDF-g-PEGA membranes with various grafting ratio (esterification reaction time=4 h) and esterification reaction time (G_R=15 wt%). The pristine PVDF membrane shows a high water flux before protein adsorption, and the PVDF-g-PAAc membrane exhibits a small water flux due to the coverage of large amount of PAAc chains (Table 2). Further incorporation of PEG chains onto the PVDF-g-PAAc membrane could not only improve the substantially decreased water flux, but also could immobilize the required hydrophilic properties. As shown in Fig. 7, the water flux decreases slightly with the increase of the grafting ratio, which could be attributed to the increased excluded volume of the hydrated PEGA chains on the membrane. However, the water flux increased a little when the grafting ratio was up to 16.9 wt%, which is probably caused by the damage to the membrane pore structure. Meanwhile, the increased water flux could be obtained by the increased esterification reaction time. It could be ascribed to the improvement of the hydrophilicity of the membrane. After being exposed to the 10 mg/ml of BSA solution for 24 h at 25 °C, the water flux of the unmodified PVDF membrane decreased to 558.7 L/m^2/h, only 44% of the original membrane. Differently, the surface modified membrane shows outstanding anti-fouling property with the increase of the grafting ratio and esterification reaction time. The water flux after protein adsorption is almost the same as before, indicating that the grafted PEGA chains on the membrane can effectively block the adsorption and deposition of the protein on the membrane surface. Thus, it could expand the fouling resistance and life-span of the membrane [36].

For PVDF-g-PEGA membranes with various esterification reaction time (G_R=15 wt%), the permeation flux of BSA solution (2 mg/ml) was determined. As shown in Fig. 8, the introduction of the PEGA chains on the membrane surface can effectively reduce the

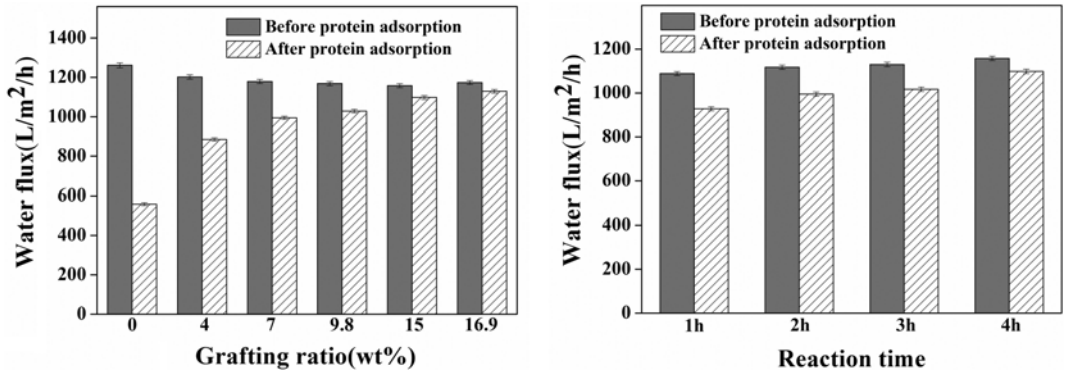

Fig. 7. Water flux of pristine and surface modified membranes before and after protein fouling with various grafting ratio and esterification reaction time.

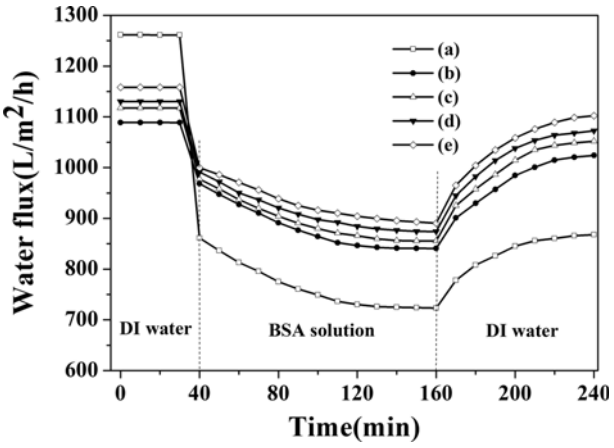

Fig. 8. Permeate flux decline behavior of (a) PVDF membrane, PVDF-g-PEGA membranes with esterification reaction time (G_R=15 wt%) of 1 h (b), 2 h (c), 3 h (d) and 4 h (e).

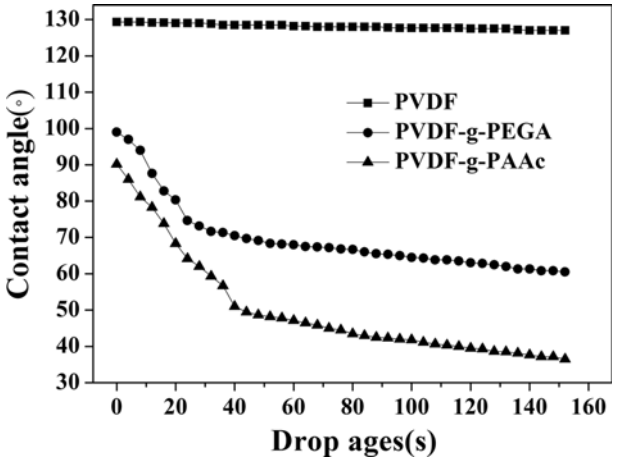

Fig. 9. The dynamic contact angle of the original and prepared PVDF membranes.

degree of the flux decline. Meanwhile, the high water flux recovery of the PVDF-g-PEGA membranes was observed at later stage of the filtration, which illustrates that the membrane modified in this work exhibits excellent antifouling performance.

4. Dynamic Contact Angle

The hydrophilicity of the PVDF membrane was characterized by the transient pure water contact angle of the membrane surface [37]. The contact angle of the PVDF-g-PAAc membrane surface drops to 36.5°, while that of PVDF-g-PEGA membrane surface drops to 60.5° within the contact time (Fig. 9). Interestingly, the data of the PVDF-g-PAAc membrane were dramatically lower than that of the original membrane and PVDF-g-PEGA membrane, indicating that the PAAc grafted membrane has a significant improvement in hydrophilicity. The possible explanation is that the carboxyl is a strong hydrophilic group, and the coordination numbers with the water molecules are up to 5 [38], while the hydroxyl groups formed on PVDF-g-PEGA membrane exhibit a weaker hydrophilicity because the maximum coordination number with the water molecules is 3. However, the incorporation of PEG chains onto the membrane surface can effectively reduce the extent of the decreased water flux caused by membrane pores blockage with massive PAAc chains, and meanwhile, PEGA chains are capable of significantly enhancing the membrane anti-fouling property. In this work, PAAc grafted onto the membrane surface can provide a reaction site for PEG; therefore, a PVDF membrane with hydrophilic and anti-fouling performance was achieved.

CONCLUSIONS

A novel method for the hydrophilic modification of PVDF membrane was proposed. The modification method could be easily carried out by a two-step polymerization reaction. The results of ATR-FTIR, XPS and SEM demonstrated that PAAc and PEG were successfully grafted onto the PVDF membrane. PVDF-g-PEGA membranes prepared using this method showed outstanding hydrophilic and anti-protein fouling performance. The protein adsorption on the modified PVDF membrane with the grafting ratio of 16.9 wt% decreased from 49 μg/cm^2 to 4 μg/cm^2. Compared with the pristine PVDF membrane, the water flux of the PVDF-g-PEGA membrane after protein fouling showed reduced degree of flux decline. These results indicate that the modified PVDF membrane could effectively prevent the protein adsorption on the membrane. The dynamic contact angle experiments show that the PVDF-g-PEGA membrane has highly hydrophilicity with the contact angle decreased from 130° of the pristine membrane to 60.5°. It is envisioned that the method proposed in this work may provide a novel idea for the modification of PVDF membranes. And the hydrophilic and low-fouling membrane achieved using this method can favor wide-range applications of PVDF membrane in the biomedical filtration and protein separation processes.

ACKNOWLEDGEMENT

The authors are grateful for the financial support received from the Key Technology R&D Program of Shanghai Committee of Science and Technology in China (14231201503), Shanghai Union Program (LM201249), 2013 Special Project of the Development and Industrialization of New Materials of National Development and Reform Commission in China (20132548) and the Key Technology R&D Program of Jiangsu Committee of Science and Technology in China (BE2013031).

REFERENCES

1. F. Liu, N. A. Hashim, Y. Liu, M. R. M. Abed and K. Li, *J. Membr. Sci.*, **375**, 1 (2011).
2. J. Liu, X. Lu, J. Li and C. Wu, *J. Polym. Res.*, **21**, 568 (2014).
3. G. D. Kang and Y. M. Cao, *J. Membr. Sci.*, **463**, 145 (2014).
4. D. Sun, P. Yang, L. Li, H. H. Yang and B. B. Li, *Korean J. Chem. Eng.*, **31**, 1877 (2014).
5. H. H. Park, C. W. Lim, H. D. Jo, W. K. Choi and H. K. Lee, *Korean J. Chem. Eng.*, **24**, 693 (2007).
6. K. M. Kim, L. R. Hepowit, J. C. Kim, Y. G. Lee and J. M. Ko, *Korean J. Chem. Eng.*, **32**, 717 (2015).
7. F. Liu, M. R. M. Abed and K. Li, *Chem. Eng. Sci.*, **66**, 27 (2011).

8. Y. Chang, C. Y. Ko, Y. J. Shih, D. Quémener, A. Deratani, T. C. Wei, D. M. Wang and J. Y. Lai, *J. Membr. Sci.*, **345**, 160 (2009).
9. M. Kemell, E. Färm, M. Ritala and M. Leskelä, *Eur. Polym. J.*, **44**, 3564 (2008).
10. A. Venault, Y. H. Liu, J. R. Wu, H. S. Yang, Y. Chang, J. Y. Lai and P. Aimar, *J. Membr. Sci.*, **450**, 340 (2014).
11. D. Rana and T. Matsuura, *Chem. Rev.*, **110**, 2448 (2010).
12. N. Pezeshk and R. M. Narbaitz, *Desalination*, **287**, 247 (2012).
13. F. Liu, Y. Y. Xu, B. K. Zhu, F. Zhang and L. P. Zhu, *J. Membr. Sci.*, **345**, 331 (2009).
14. N. A. Hashim, F. Liu and K. Li, *J. Membr. Sci.*, **345**, 134 (2009).
15. N. A. Ochoa, M. Masuelli and J. Marchese, *J. Membr. Sci.*, **226**, 203 (2003).
16. J. Hester and A. Mayes, *J. Membr. Sci.*, **202**, 119 (2002).
17. S. Boributh, A. Chanachai and R. Jiraratananon, *J. Membr. Sci.*, **342**, 97 (2009).
18. M. Z. Li, J. H. Li, X. S. Shao, J. Miao, J. B. Wang, Q. Q. Zhang and X. P. Xu, *J. Membr. Sci.*, **405-406**, 141 (2012).
19. Y. Chang, W. J. Chang, Y. J. Shih, T. C. Wei and G. H. Hsiue, *ACS Appl. Mater. Interfaces*, **3**, 1228 (2011).
20. Y. Chang, Y. J. Shih, R. C. Ruaan, A. Higuchi, W. Y. Chen and J. Y. Lai, *J. Membr. Sci.*, **309**, 165 (2008).
21. M. Zhang, Q. T. Nguyen and Z. Ping, *J. Membr. Sci.*, **327**, 78 (2009).
22. D. Brewis, I. Mathieson, I. Sutherland, R. Cayless and R. Dahm, *Int. J. Adhes. Adhes.*, **16**, 87 (1996).
23. G. Ross, J. Watts, M. Hill and P. Morrissey, *Polymer*, **41**, 1685 (2000).
24. Y. J. Byun, J. H. Kim and S. S. Kim, *Desalin. Water. Treat.*, **51**, 5371 (2013).
25. A. Rahimpour, S. Madaeni, S. Zereshki and Y. Mansourpanah, *Appl. Surf. Sci.*, **255**, 7455 (2009).
26. L. Ying, P. Wang, E. Kang and K. Neoh, *Macromolecules*, **35**, 673 (2002).
27. P. Wang, K. Tan, E. Kang and K. Neoh, *J. Membr. Sci.*, **195**, 103 (2002).
28. B. Peng, Y. Y. Li, Z. G. Zhao, Y. M. Chen and C. C. Han, *J. Appl. Polym. Sci.*, **130**, 3112 (2013).
29. G. Kang, M. Liu, B. Lin, Y. Cao and Q. Yuan, *Polymer*, **48**, 1165 (2007).
30. Q. F. Liu, C. H. Lee and H. Kim, *Sep. Sci. Technol.*, **45**, 1209 (2010).
31. A. Bottino, G. Capannelli and A. Comite, *J. Membr. Sci.*, **273**, 20 (2006).
32. M. G. Zhang, Q. T. Nguyen and Z. H. Ping, *J. Membr. Sci.*, **327**, 78 (2009).
33. M. Tamura, T. Uragami and M. Sugihara, *Polymer*, **22**, 829 (1981).
34. Y. P. Zhao, H. Y. Zhao, L. Chen, X. Feng, Q. S. Zhang, J. M. Wang and R. Zhang, *J. Polym. Res.*, **20**(1), 1 (2013).
35. C. C. Hsu, C. S. Wu and Y. L. Liu, *J. Membr. Sci.*, **450**, 257 (2014).
36. Y. H. Zhao, B. K. Zhu, L. Kong and Y. Y. Xu, *Langmuir*, **23**, 5779 (2007).
37. X. J. Zhao, J. Cheng, S. J. Chen, J. Zhang and X. L. Wang, *Colloid. Polym. Sci.*, **288**, 1327 (2010).
38. L. X. Gu and Z. F. Liu, Hydrophilic fibers (Chinese), China Petrochemical Press, Beijing (1997).